The Orbit of GW170817 Was Inclined by Less Than 28° to the Line of Sight

Mandel, Ilya

DOI:
10.3847/2041-8213/aaa6c1

The Astrophysical Journal Letters, 853:L12 (3pp), 2018 January 20 https://doi.org/10.3847/2041-8213/aaa6c1

The Orbit of GW170817 Was Inclined by Less Than 28° to the Line of Sight

Ilya Mandel
Institute of Gravitational Wave Astronomy and School of Physics and Astronomy, University of Birmingham, Birmingham B15 2TT, UK
imandel@star.sr.bham.ac.uk
Received 2017 December 13; revised 2018 January 8; accepted 2018 January 9; published 2018 January 23

Abstract

We combine the gravitational-wave measurement of the effective distance to the binary neutron star merger GW170817, the redshift of its host galaxy NGC 4993, and the latest Hubble constant measurement from the Dark Energy Survey to constrain the inclination between the orbital angular momentum of the binary and the line of sight to $18° \pm 8°$ (less than 28° at 90% confidence). This provides a complementary constraint on models of potential afterglow observations.

Key words: binaries: close – gravitational waves – stars: neutron

1. Introduction

Gravitational waves from the coalescence of two neutron stars, GW170817, were detected by the advanced LIGO (Aasi et al. 2015) and Virgo (Acernese et al. 2015) gravitational-wave observatories on 2017 August 17 (Abbott et al. 2017c). A short gamma-ray burst was observed by *Fermi* less than 2 s later (Abbott et al. 2017b). These detections initiated a campaign of electromagnetic observations that identified the transient source and localized it to the host galaxy NGC 4993 (Abbott et al. 2017d and references therein).

For a nearly face-on binary located nearly overhead a gravitational-wave detector, the gravitational-wave signal amplitude scales as $\cos \iota / D_L$, where D_L is the luminosity distance to the source and ι is the inclination angle to the line of sight (0° for a face-on and 180° for a face-off binary). Gravitational-wave observations measure the signal amplitude to a fractional accuracy of $\sim 1/\rho$, where the signal-to-noise ratio ρ is approximately 32 for GW170817 (Abbott et al. 2017c). However, the inclination–distance degeneracy prevents a precise inclination measurement, and the viewing angle can only be constrained to be below 55° from gravitational-wave observations alone (Abbott et al. 2017c).

This inclination–distance degeneracy, inherent in gravitational-wave inference (e.g., Veitch et al. 2012), can be broken with the aid of an independent distance measurement. The observed recession velocity of the host galaxy, NGC 4993 (e.g., Hjorth et al. 2017), combined with a precise value of the Hubble constant, provides such a measurement.

The most recent measurement of the Hubble constant by the Dark Energy Survey (DES) team yields a value of $H_0 = 67.2^{+1.2}_{-1.0}$ km s^{-1} Mpc^{-1} (DES Collaboration et al. 2017). This is very similar to the H_0 value inferred from Planck data (Planck Collaboration et al. 2016). The DES team also combines results with four other statistically independent H_0 measurements—Planck and SPTpol (Henning et al. 2017), which use independent CMB information; SH0ES (Riess et al. 2016), which is based on standard candles provided by type IA supernovae; and H0LiCOW (Bonvin et al. 2017), which uses time delays between images of strongly lensed variable quasars—to yield the very precise value of $H_0 = 69.1^{+0.4}_{-0.6}$ km s^{-1} Mpc^{-1} (DES Collaboration et al. 2017).

Abbott et al. (2017a) combined the LIGO/Virgo distance data with the observed redshift of the host galaxy NGC 4993 to obtain an independent measurement of H_0. Here, we reverse their approach: we take the data behind Figure 2 of Abbott et al. (2017a), which includes posterior samples in the two-dimensional H_0–$\cos \iota$ space and resample them according to the tighter, independent H_0 measurements in order to obtain a posterior distribution on ι, where we map ι onto the range $0° \leqslant \iota \leqslant 90°$.

2. Results

In the Bayesian framework, we marginalize the joint posterior probability distribution on ι and H_0 given both the gravitational-wave data $\boldsymbol{d}_{\rm GW}$ and independent data $\boldsymbol{d}_{H_0}$ that provide improved knowledge of H_0:

$$p(\iota|\text{data}) = \int p(\iota, H_0|\boldsymbol{d}_{\rm GW}, \boldsymbol{d}_{H_0}) dH_0. \tag{1}$$

We use the existing joint posterior computed from gravitational-wave observations by Abbott et al. (2017a):

$$p(\iota, H_0|\boldsymbol{d}_{\rm GW}) \propto \pi_{\rm LVC}(\iota)\pi_{\rm LVC}(H_0)p(\boldsymbol{d}_{\rm GW}|\iota, H_0), \tag{2}$$

where $\pi_{\rm LVC}$ denote the priors used by Abbott et al. (2017a) with $\pi_{\rm LVC}(H_0) \propto 1/H_0$. Therefore,

$$\begin{aligned} p(\iota, H_0|\boldsymbol{d}_{\rm GW}, \boldsymbol{d}_{H_0}) &\propto \pi_{\rm LVC}(\iota)p(H_0|\boldsymbol{d}_{H_0})p(\boldsymbol{d}_{\rm GW}|H_0, \iota) \\ &\propto p(\iota, H_0|\boldsymbol{d}_{\rm GW})\frac{p(H_0|\boldsymbol{d}_{H_0})}{\pi_{\rm LVC}(H_0)}, \end{aligned} \tag{3}$$

where $p(H_0|\boldsymbol{d}_{H_0})$ is the distribution of H_0 inferred from independent observations.

Figure 1 shows the posterior on ι re-weighted by the H_0 measurements from DES Collaboration et al. (2017). Specifically, we re-weighted the data from Abbott et al. (2017a) by the ratio $p(H_0|\boldsymbol{d}_{H_0})/\pi_{\rm LVC}(H_0)$. We approximated the DES measurement $p(H_0|\boldsymbol{d}_{H_0})$ as a normal distribution with mean 67.3 km s^{-1} Mpc^{-1} and standard deviation 1.1 km s^{-1} Mpc^{-1}. The inclination angle ι is constrained to be $18° \pm 8°$ with a 90%-confidence upper limit of 28°.

If instead the combined H_0 value from five measurements is used (DES Collaboration et al. 2017), approximated as a normal distribution with mean 69.0 km s^{-1} Mpc^{-1} and standard deviation 0.5 km s^{-1} Mpc^{-1}, we obtain an inclination angle $\iota = 20° \pm 8°$ with a 90%-confidence upper limit of 30°. These constraints are summarized in Table 1.

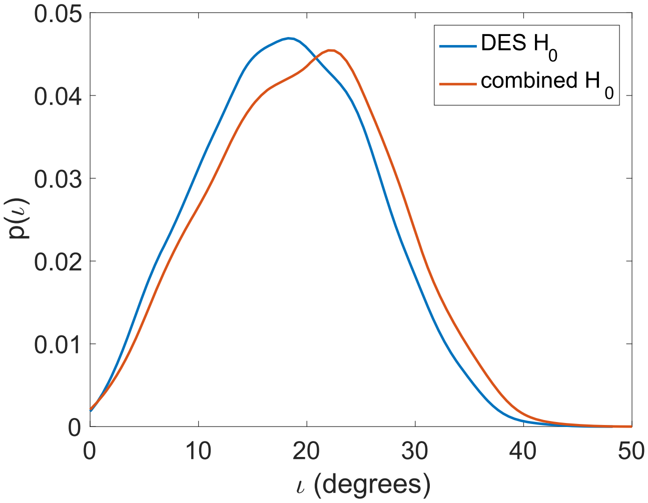

Figure 1. Probability distribution on the orbital inclination angle ι of GW170817, obtained by combining the distance and inclination inferred from the gravitational-wave signal, the host galaxy redshift, and an independent measurement of the Hubble constant. The blue curve is based on the DES measurement of H_0, while the red curve is based on a combination of five statistically independent H_0 measurements (DES Collaboration et al. 2017).

Table 1
The Inferred Value of the Inclination Angle ι (with 90% Upper Limits in Parentheses) for Each of the H_0 Observations as Described in the Text

H_0 Source	H_0 (km s^{-1} Mpc^{-1})	ι (degrees)
DES-only[a]	$67.2^{+1.2}_{-1.0}$	18 ± 8 (28)
DES+$v_{\rm pec}$[b]	...	(31)
Combined[a]	$69.1^{+0.4}_{-0.6}$	20 ± 8 (30)
SHOES[c]	73.24 ± 1.74	25 ± 8 (35)

Notes.
[a] DES Collaboration et al. (2017).
[b] H_0 as above, with 100 km s^{-1} peculiar velocity offset assumed.
[c] Riess et al. (2016).

Our constraint on low inclination angles is not informative: as $\iota \to 0$, the inferred posterior probability distribution on ι is consistent with the prior, $p(\iota) \propto \sin\iota$, which disfavors very small inclination angles. Pian et al. (2017) point out that the a priori probability for $\iota < 26°$ is only 10%.[1] However, as pointed out by Guidorzi et al. (2017), low values of ι are ruled out by electromagnetic observations, which indicate that the Earth is neither in the jet nor too close to the jet, given the $\gtrsim$10 day delay times before radio and X-ray afterglows were detected (Hallinan et al. 2017; Troja et al. 2017).

3. Discussion

The DES Collaboration et al. (2017) and Planck Collaboration et al. (2016) values of the Hubble constant are significantly lower than the value inferred from type Ia supernova and the local distance ladder, $H_0 = 73.24 \pm 1.74$ km s^{-1} Mpc^{-1} (Riess et al. 2016). The latter value would yield $\iota = 25° \pm 8°$ with a 90%-confidence upper limit of 35°. However, while the Planck value is based on cosmic microwave background measurements and its discrepancy with the Riess et al. (2016) value could conceivably be due to a failing of the standard Λ CDM cosmology, the DES value is ultimately based on low-redshift galaxy clustering and weak lensing observations, but without the potential systematics inherent in calibrating a distance ladder.

The peculiar velocity of NGC 4993 relative to the Hubble flow can affect the conversion of its redshift into distance. Abbott et al. (2017a) consider a variation in which the uncertainty on the peculiar velocity is increased to 250 km s^{-1} from the nominal 150 km s^{-1}; this has virtually no effect (see their extended Table I). We also consider a systematic shift in the peculiar velocity by 100 km s^{-1} in addition to this velocity uncertainty. This corresponds to a 3% shift in the velocity, and hence a 3% change in the distance for a given value of H_0. The resulting 3% shift in $\cos\iota$ could move the 90% upper limit on ι from 28° to 31°.

Our maximum inclination angle constraint is significantly tighter than the constraint from gravitational-wave measurements alone, less than 55° at 90% confidence (Abbott et al. 2017c).[2] This complementary constraint can aid in the interpretation of the electromagnetic transient associated with this binary neutron star merger. In particular, it strongly limits the available parameter space for models of observed electromagnetic signatures, ruling out several proposals. For example, we can rule out the preferred model of Kim et al. (2017), which explains radio observations by appealing to an observing angle of 41°. The preferred "top-hat" jet model of Lazzati et al. (2017) with the same observing angle can also be ruled out, though their structured jet model is consistent with the inclination constraint presented here. The model of Evans et al. (2017), which prefers an observing angle of $\approx$30°, is only marginally consistent with the maximum allowed inclination value. The models of Nicholl et al. (2017), Troja et al. (2017), Alexander et al. (2017), Margutti et al. (2017), Perego et al. (2017), and Mooley et al. (2017) are consistent with the constraint presented here for only part of their parameter space; adding this additional constraint could allow for more precise estimates of other free parameters in these models. Other models consistent with the maximum inclination value presented here include Fraija et al. (2017) and Haggard et al. (2017).

As another example application, we can translate the threshold on ι into a constraint on the jet energy and the density of the surrounding material. The afterglow peak is expected at

$$t_{\rm peak} \sim 70 \left(\frac{E}{10^{51}\,{\rm erg}}\right)^{1/3} \left(\frac{n}{1\,{\rm cm}^{-3}}\right)^{-1/3} \theta_{\rm obs}^2\ {\rm days} \tag{4}$$

after the merger (Granot et al. 2017), where E is the jet kinetic energy, n is the interstellar medium density, and $\theta_{\rm obs}$ is the observing angle in radians. We assume that the jet is perpendicular to the binary's orbital plane, so $\theta_{\rm obs} = \iota$. The constraint on ι provided here then yields

$$\frac{E}{10^{50}\,{\rm erg}} \frac{10^{-4}\,{\rm cm}^{-3}}{n} \gtrsim \left(\frac{t_{\rm peak}}{170\ {\rm days}}\right)^3 \left(\frac{\iota}{28°}\right)^{-6}. \tag{5}$$

The isotropic-equivalent energy of the jet, $E_{\rm iso} \sim 2E/\theta_0^2$ where θ_0 is the jet opening angle, has been observed to range from 3×10^{49} to 3×10^{52} erg, while the inferred circum-merger density n ranges from $\sim 10^{-4}$ to ~ 1 cm^{-3} in on-axis events (Fong et al. 2015). The jet opening angle has been estimated

[1] The a priori probability for $\iota < 26°$ rises to 30% if selection effects from gravitational-wave searches are included, due to mild on-axis beaming of gravitational waves.

[2] A similar constraint to the one obtained here was made by assuming the Planck value of H_0 by Abbott et al. (2017c).

from jet breaks and from the requirement of matching short gamma-ray burst rates to binary neutron star merger rates to be $\theta_0 \sim 10°$ (Fong & Berger 2013; Fong et al. 2015). Therefore, the observations of a continuing afterglow lasting beyond 100 days after the merger (Lazzati et al. 2017; Lyman et al. 2017; Mooley et al. 2017; Ruan et al. 2017) indicate that the merger happened in a very low-density environment, $n \lesssim 10^{-4}$ cm^{-3}. Alternatively, they could indicate that there is limited or no sideways expansion of the jet, which would increase the peak time for a given choice of E and n by a factor of $(\theta_{\rm obs}/\theta_0)^{2/3}$ relative to Equation (4), therefore relaxing the constraint on the maximum n obtained here by a factor of $(\theta_{\rm obs}/\theta_0)^2$; even then, the rise of the afterglow should not extend beyond ~550 days after merger for $n \gtrsim 10^{-4}$ cm^{-3}.

We thank Christopher Berry, Jens Hjorth, and Nial Tanvir for useful discussions. We particularly thank Will Farr for contributing to the formulation of this work; unfortunately, he did not wish to be an author because of restrictions required by the LIGO Scientific Collaboration policies. I.M. is partially supported by STFC.

ORCID iDs

Ilya Mandel https://orcid.org/0000-0002-6134-8946

References

Aasi, J., Abbott, B. P., Abbott, R., et al. 2015, CQGra, 32, 074001
Abbott, B. P., Abbott, R., Abbott, T. D., et al. 2017a, Natur, 551, 85
Abbott, B. P., Abbott, R., Abbott, T. D., et al. 2017b, ApJL, 848, L13
Abbott, B. P., Abbott, R., Abbott, T. D., et al. 2017c, PhRvL, 119, 161101
Abbott, B. P., Abbott, R., Abbott, T. D., et al. 2017d, ApJL, 848, L12
Acernese, F., Agathos, M., Agatsuma, K., et al. 2015, CQGra, 32, 024001
Alexander, K. D., Berger, E., Fong, W., et al. 2017, ApJL, 848, L21
Bonvin, V., Courbin, E., Suyu, S. H., et al. 2017, MNRAS, 465, 4914
DES Collaboration, Abbott, T. M. C., Abdalla, F. B., et al. 2017, arXiv:1711.00403
Evans, P. A., Cenko, S. B., Kennea, J. A., et al. 2017, Sci, https://doi.org/10.1126/science.aap9580
Fong, W., & Berger, E. 2013, ApJ, 776, 18
Fong, W., Berger, E., Margutti, R., & Zauderer, B. A. 2015, ApJ, 815, 102
Fraija, N., De Colle, F., Veres, P., et al. 2017, ApJ, submitted (arXiv:1710.08514)
Granot, J., Gill, R., Guetta, D., & De Colle, F. 2017, MNRAS, submitted (arXiv:1710.06421)
Guidorzi, C., Margutti, R., Brout, D., et al. 2017, ApJL, 851, L36
Haggard, D., Nynka, M., Ruan, J. J., et al. 2017, ApJL, 848, L25
Hallinan, G., Corsi, K., Mooley, K. P., et al. 2017, Sci, https://doi.org/10.1126/science.aap9855
Henning, J. W., Sayre, J. T., Reichardt, C. L., et al. 2017, ApJ, submitted (arXiv:1707.09353)
Hjorth, J., Levan, A. J., Tanvir, N. R., et al. 2017, ApJL, 848, L31
Kim, S., Schulze, S., Resmi, L., et al. 2017, ApJL, 850, L21
Lazzati, D., Perna, R., Morsony, B. J., et al. 2017, arXiv:1712.03237
Lyman, J., Lamb, G. P., Levan, A. J., et al. 2017, arXiv:1801.02669
Margutti, R., Berger, E., Fong, W., et al. 2017, ApJL, 848, L20
Mooley, K. P., Nakar, E., Hotokezaka, K., et al. 2017, arXiv:1711.11573
Nicholl, M., Berger, E., Kasen, D., et al. 2017, ApJL, 848, L18
Perego, A., Radice, D., & Bernuzzi, S. 2017, ApJL, 850, L37
Pian, E., D'Avanzo, P., Benetti, S., et al. 2017, Natur, 551, 67
Planck Collaboration, Ade, P. A. R., Aghanim, N., et al. 2016, A&A, 594, A13
Riess, A. G., Macri, L. M., Hoffmann, S. L., et al. 2016, ApJ, 826, 56
Ruan, J. J., Nynka, M., Haggard, D., Kalogera, V., & Evans, P. 2017, ApJL, 853, L4
Troja, E., Piro, L., van Eerten, H., et al. 2017, Natur, 551, 71
Veitch, J., Mandel, I., Aylott, B., et al. 2012, PhRvD, 85, 104045